Supporting Information

Quaternary Morpholinium-Mediated Defect Control in High-Performance Perovskite Solar Cells

Shengnan Wang,[a] Ranran Xu,[a] Fengqiao Xu,[a] Weidong Lin,[b] Zhixiao Qin,*[c] Taiyang Zhang,*[b] Yongbing Lou*[a]

[a]School of Chemistry and Chemical Engineering, Southeast University, Nanjing 211189, China

[b]School of Chemical and Environmental Engineering, Shanghai Institute of Technology, 100 Haiquan Road, Shanghai 201418, China

[c]Shanghai Pvsktech Co., Ltd., Shanghai, China

Corresponding Authors

Zhixiao Qin, Email: zhixiao.qin@pvsktech.com

Taiyang Zhang, Email: taiyangzhang@sit.edu.cn.

Yongbing Lou, Email: lou@seu.edu.cn.

Methods

Materials

FTO glass substrates were purchased from Suzhou ShangYang Solar Technology. Lead iodide (PbI_2, 99.999%), formamidinium iodide (FAI, 99.8%), methylamine iodide (MAI, 99.9%), cesium iodide (CsI, 99.98%), methylammonium chloride (MACl, 99.99%), fullerene (C_{60}, 99.9%) and 2,9-dimethyl-4,7-diphenyl-1,10-Phenanthroline (BCP, 99.99%) were purchased from Xi'an Yuri Solar CO., Ltd. [4-(3,6-dimethyl-9H-carbazol-9-yl)butyl]phosphonic acid (Me-4PACz, 98%) and NiO_x were purchased from TCI Chemicals. The 4-ethyl-4-methylmorpholinium bromide (EMMorBr, 99%) was purchased from Shanghai Aladdin Biochemical Technology Co., Ltd. N,N-Dimethylformamide (DMF, 99.8%), dimethyl sulfoxide (DMSO, 99.7%), chlorobenzene (CB, 99.9%), isopropanol (IPA, 99.5%) and ethanol (EtOH, 99.5%) were purchased from J&K Scientific Ltd.

Preparation of perovskite solutions

1.5 M $FA_{0.85}MA_{0.1}Cs_{0.05}PbI_3$ perovskite precursor was prepared by dissolving 19.5 mg CsI, 23.8 mg MAI, 219.3 mg FAI, 726.1 mg PbI_2 (with 5% mol excess) and 15.2 mg MACl in 800 µl DMF and 200 µl DMSO. After stirring for 10 hours, the precursor solution was filtered with 0.22 µm PTFE membrane before use.

Solar cell device fabrication

Perovskite solar cells were fabricated with an p−i−n-type planar heterojunction structure consisting of FTO/NiO_x/Me-4PACz/Perovskite/EMMorBr/C_{60}/BCP/Cu. The FTO substrates (2 cm × 2 cm) were ultrasonically cleaned in soap water, deionized water, acetone and IPA in sequence for each 20 min. After drying the FTO substrates with N_2 stream, the substrates were treated with ultraviolet ozone for 15 min. Then the NiO_x layer was fabricated by spin-coating the NiO_x dispersions (5 mg mL^{-1} dispersed in deionized water) on FTO substrates at 3000 rpm for 30 s, and annealed at 150 °C for 10 min in ambient air. Then these substrates were transferred into a N_2-filled glove box. The Me-4PACz (0.5 mg mL^{-1} in ethanol) was spin-coated on NiO_x at 3000 rpm for 30 s, and annealed at 100 °C for 10 min. Then the perovskite layers were fabricated by spin-

coating 75 μL precursor solution onto the HTL at 1000 rpm for 10 s then at 5000 rpm for 30 s, with 200 μL chlorobenzene added as an anti-solvent at 5 s before spin-coating concluded. Subsequently, the film was annealed at 100 °C for 10 min. The passivation layer was fabricated by spin-coating the EMMorBr (0.9 mg mL^{-1} in IPA) on perovskite at 5000 rpm for 30 s, followed by annealing at 100 °C for 5 min. The electron transport layer (ETL) was fabricated by thermal evaporation of C_{60} (20 nm) at a rate of 0.1 Å s^{-1}. Finally, BCP (6 nm) at a rate of 0.1 Å s^{-1}, and Cu (80 nm) were thermally evaporated.

Characterization of Devices Performance.

Current density-voltage (*J-V*) characteristics of the PSCs were measured using a Keithley 2400 source measurement unit under an AM 1.5G solar simulator (Enlitech, China). The light intensity was calibrated using a KG-5 standard silicon cell, consistent with the National Photovoltaic Calibration Center. The *J-V* curves were obtained by reverse scanning (1.25 V to -0.1 V, step size of 0.03 V, with a dwelling time of 10 ms per step) and forward scanning (-0.1 V to 1.25 V, step size of 0.03 V, with a dwelling time of 10 ms per step). The effective area of the solar cell was defined by a metal mask with an area of 0.06 cm2. All *J-V* tests were conducted in ambient conditions. Additionally, external quantum efficiency (EQE) was measured by using a Keithley 2400 source meter combined with an Ocean Insight QE 65Pro fibre optic spectrometer. The steady-state maximum power conversion efficiency was collected by tracking the maximum power point under continuous illumination with a light intensity of 100 mW cm^{-2} (AM1.5G) for 300 seconds in ambient conditions. For stability test, encapsulated devices were stored in an ambient condition under 30-40% RH.

Other characterizations and measurements

The FTIR spectra were obtained by Nicolet iS50R FTIR spectrometer (Thermo Scientific Co., America). XPS measurements were performed on a Thermo ESCALAB 250XI using 100 W monochromatic Al Kα X-ray source (1486.6 eV), the binding energy scale was referenced to the adventitious carbon C 1s peak, set at 284.8 eV. The SEM images were gained by a Zeiss Ultra Plus scanning electron microscope at 10 kV operating voltage. The XRD spectra were collected on a Haoyuan DX-2800 X-ray diffractometer with a Cu Kα source. An Agilent Cary-60 UV–vis spectrophotometer

was applied for the UV–vis absorption spectra. Steady-state PL and TRPL measurements were achieved on a Horiba Scientific Delt Flex spectrometer. PL mapping images were observed using a Renishaw inVia confocal Raman microscope. An AXIS-ULTRA DLD-600W Ultra spectrometer with a He discharge lamp (ultraviolet energy at 21.22 eV) was used to record the UPS spectra. Contact angles were measured using the KSV-CAM-200 contact angle measuring instrument. The EIS and Mott-Schottky curves were acquired using a CHI660E electrochemistry workstation.

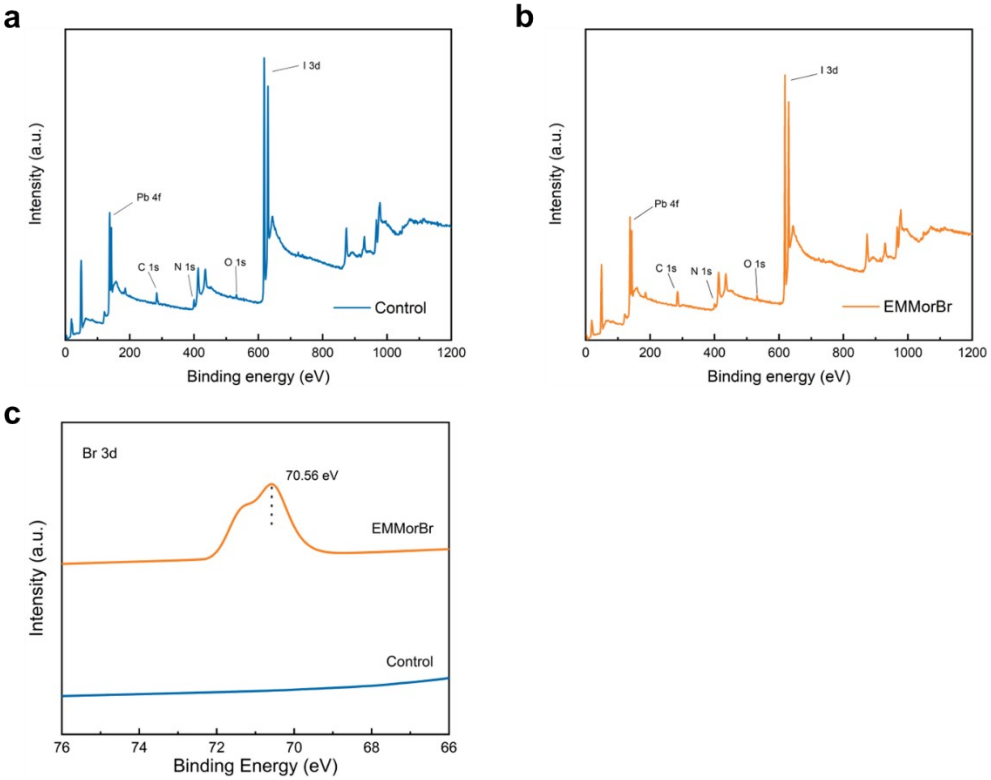

Figure S1. (a), (b) The full XPS spectra for control and EMMorBr-modified perovskite films. (c) Br 3d XPS spectra of control and EMMorBr-modified perovskite films.

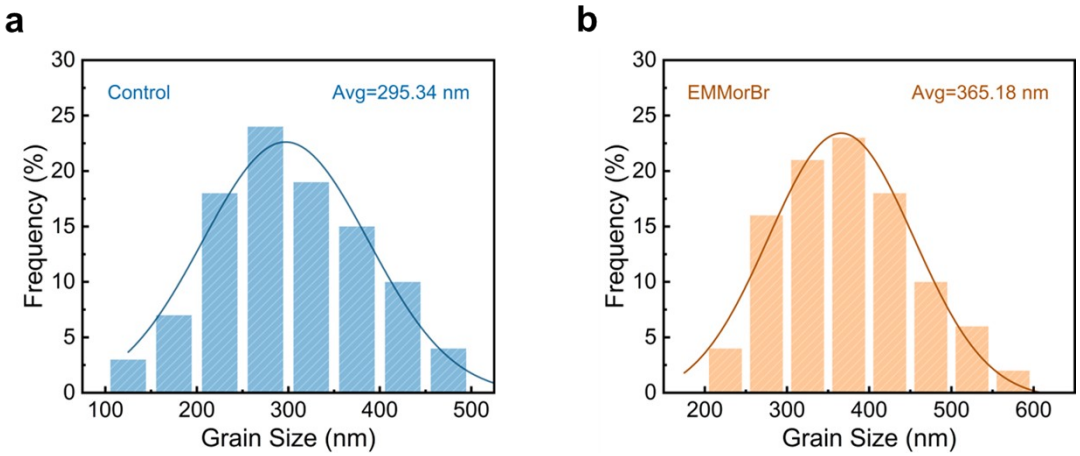

Figure S2. The corresponding grain size distribution based on top-view SEM images.

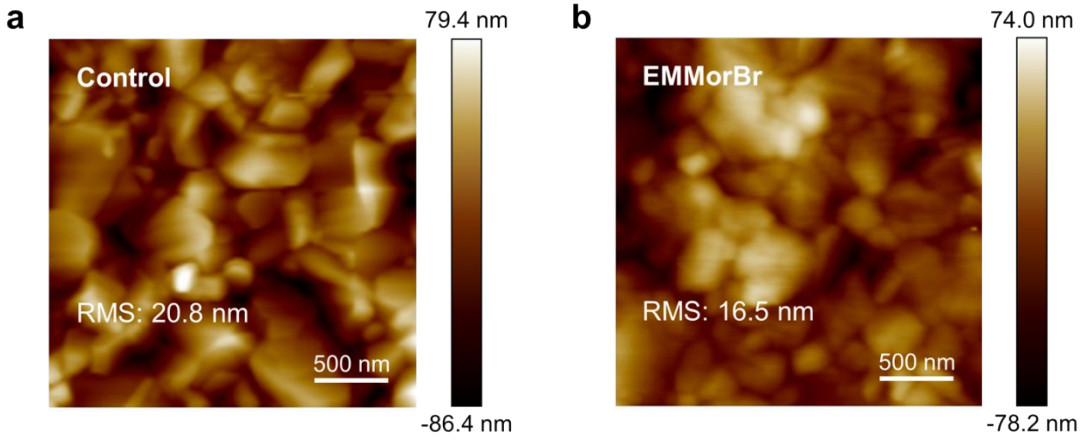

Figure S3. The AFM images of the control and EMMorBr-modified perovskite films.

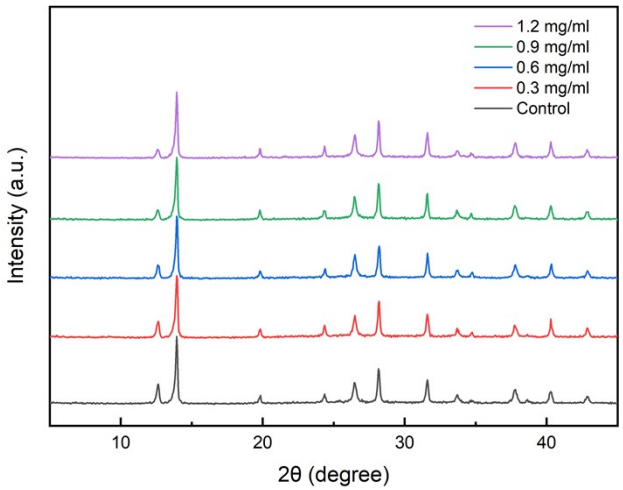

Figure S4. XRD diffractions of perovskite films with different EMMorBr concentrations.

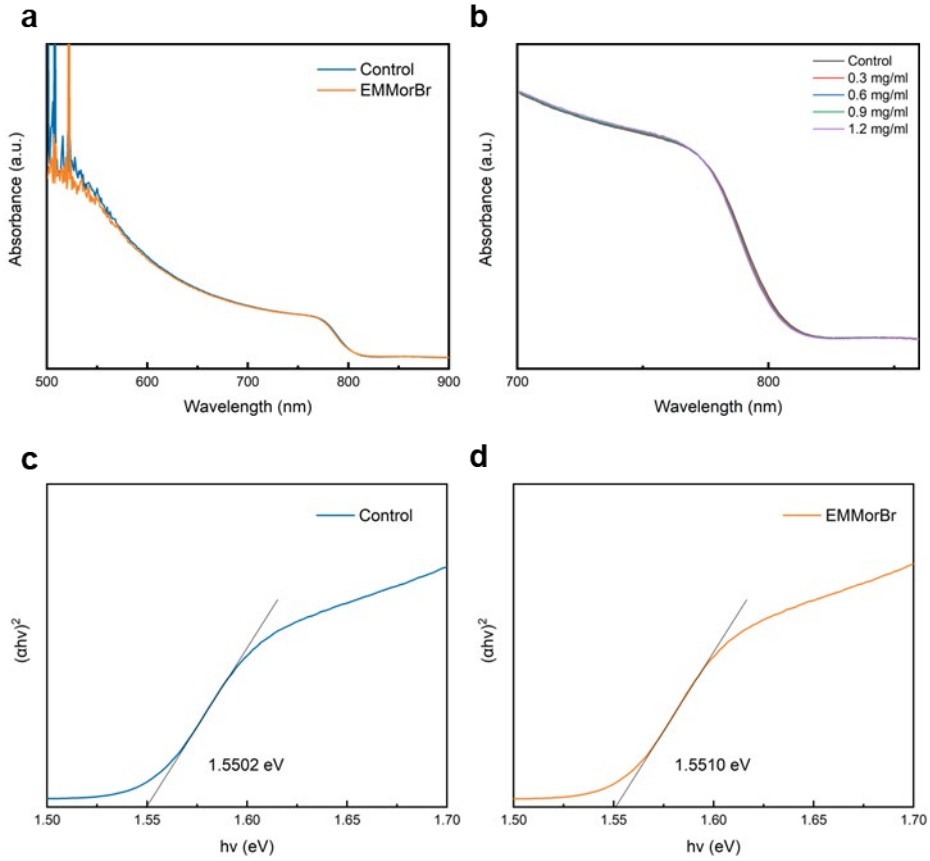

Figure S5. (a) The absorption spectra of Control, and EMMorBr-modified (0.9 mg/ml) perovskite films. (b) The absorption spectra of perovskite films modulated by different concentrations of EMMorBr. (c), (d) Tauc plots of control and EMMorBr-modified (0.9 mg/ml) perovskite films.

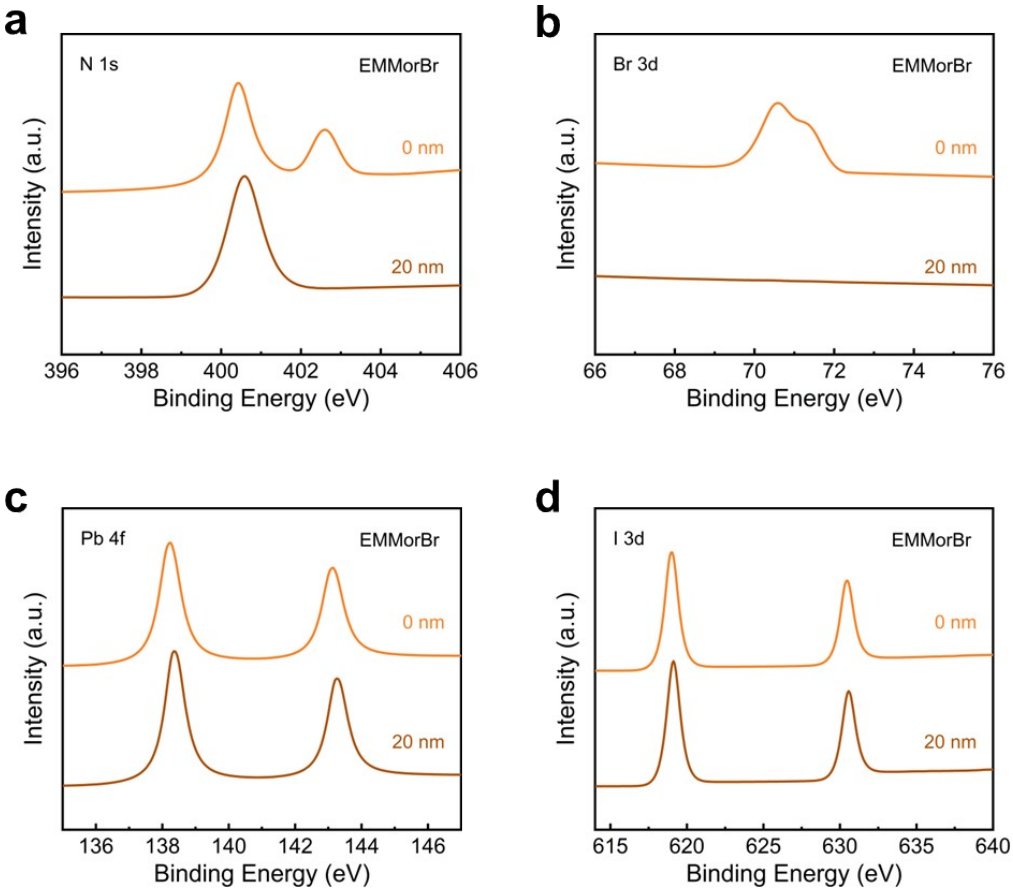

Figure S6. The XPS spectra of EMMorBr-modified perovskite films surface and after etching 20 nm.

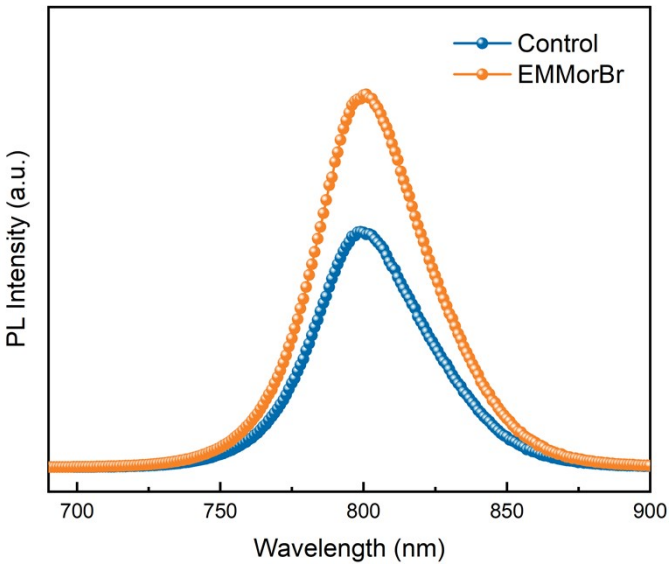

Fig S7. PL spectra of the control and EMMorBr-modified perovskite films deposited on nonconductive glass.

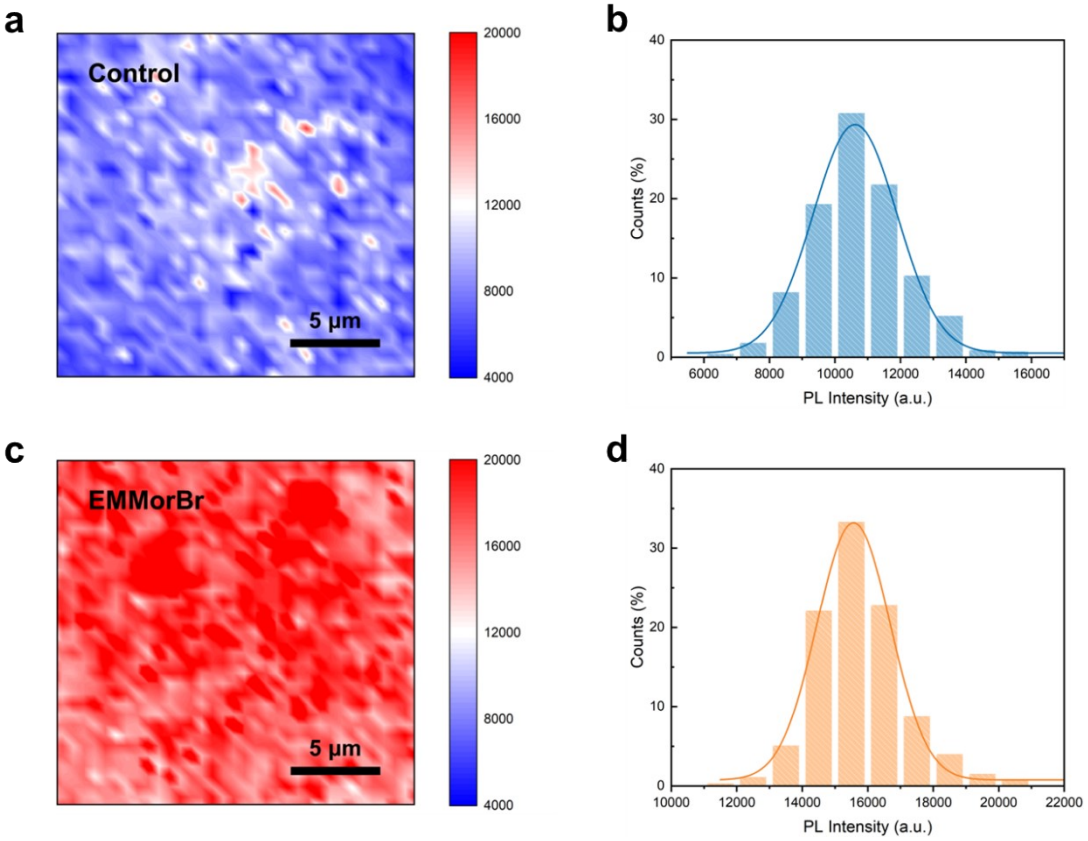

Fig S8. Histogram for PL intensity distribution from perovskite films with and without EMMorBr modification.

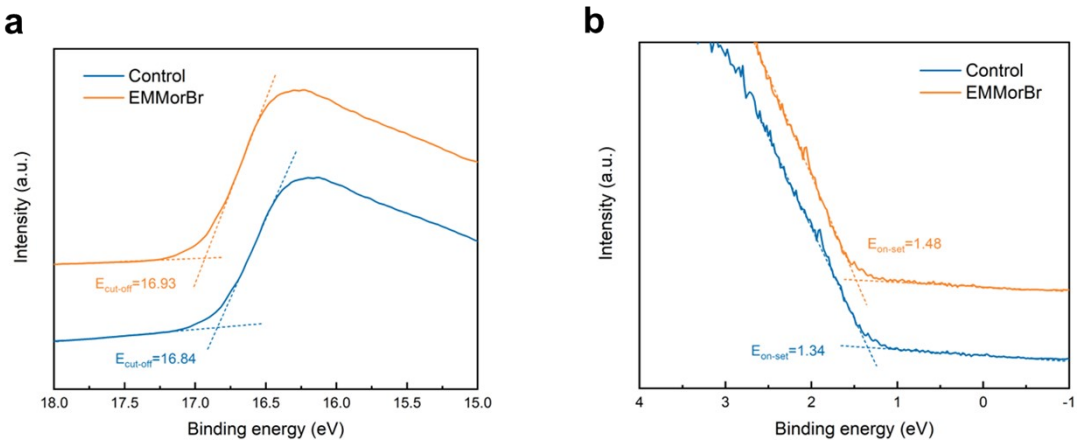

Fig S9. UPS spectra of the perovskite films with and without EMMorBr modification

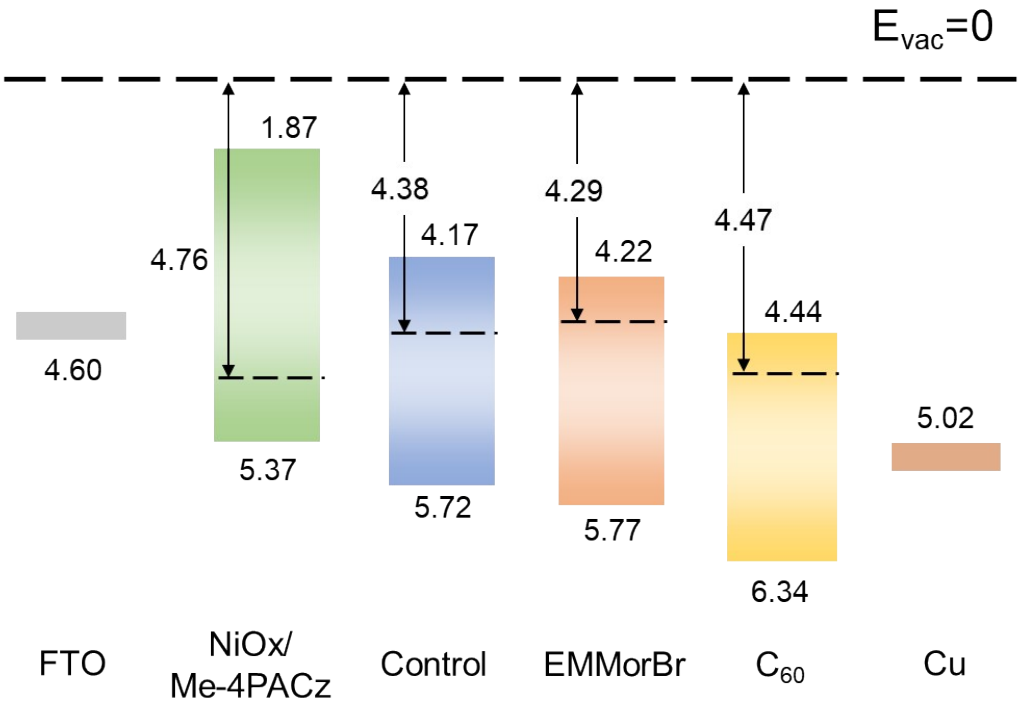

Fig S10. The energy level diagram of the control and modified devices.

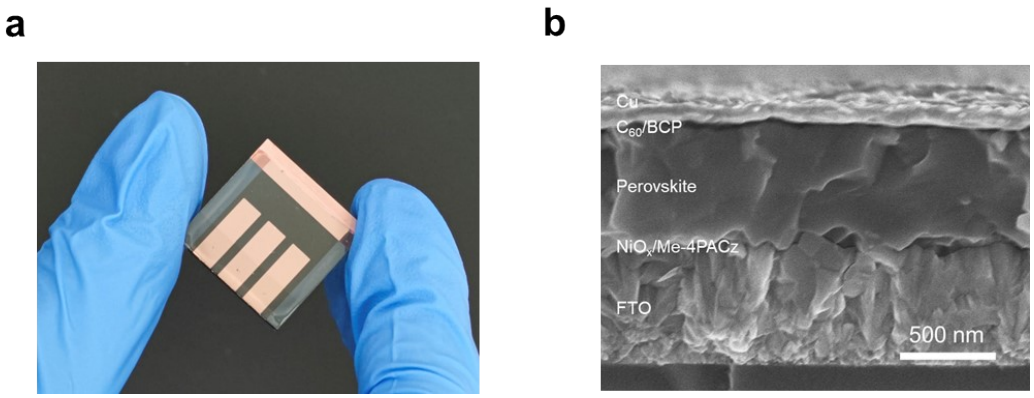

Fig S11. (a) The photograph of the champion 2 cm × 2 cm mini-module with EMMorBr modification. (b) Cross-sectional SEM image of the device structure.

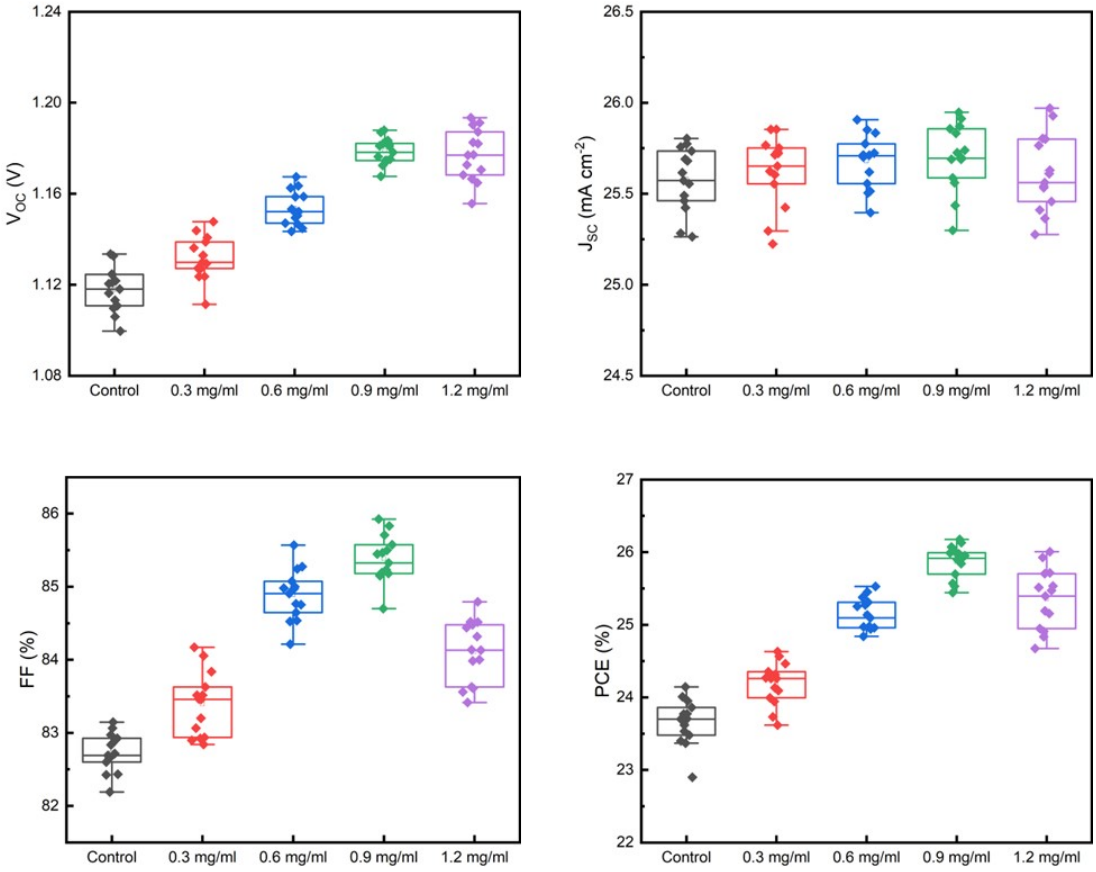

Fig S12. Statistics of V_{OC}, J_{SC}, FF and PCE of the PSCs modulated by different concentrations of EMMorBr. The statistic data were obtained from individual 14 devices for each kind of PSCs.

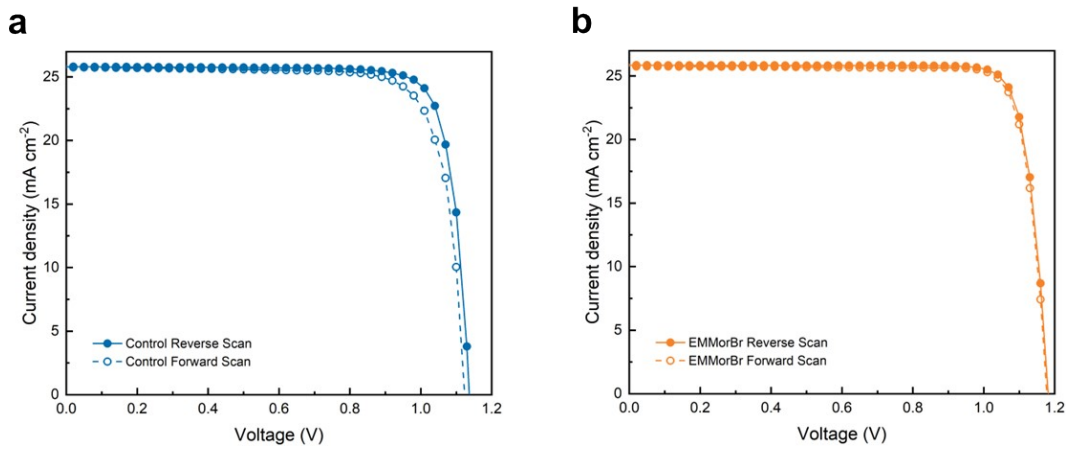

Fig S13. *J-V* curves by forward and reverse scanning of PSCs with and without EMMorBr modification.

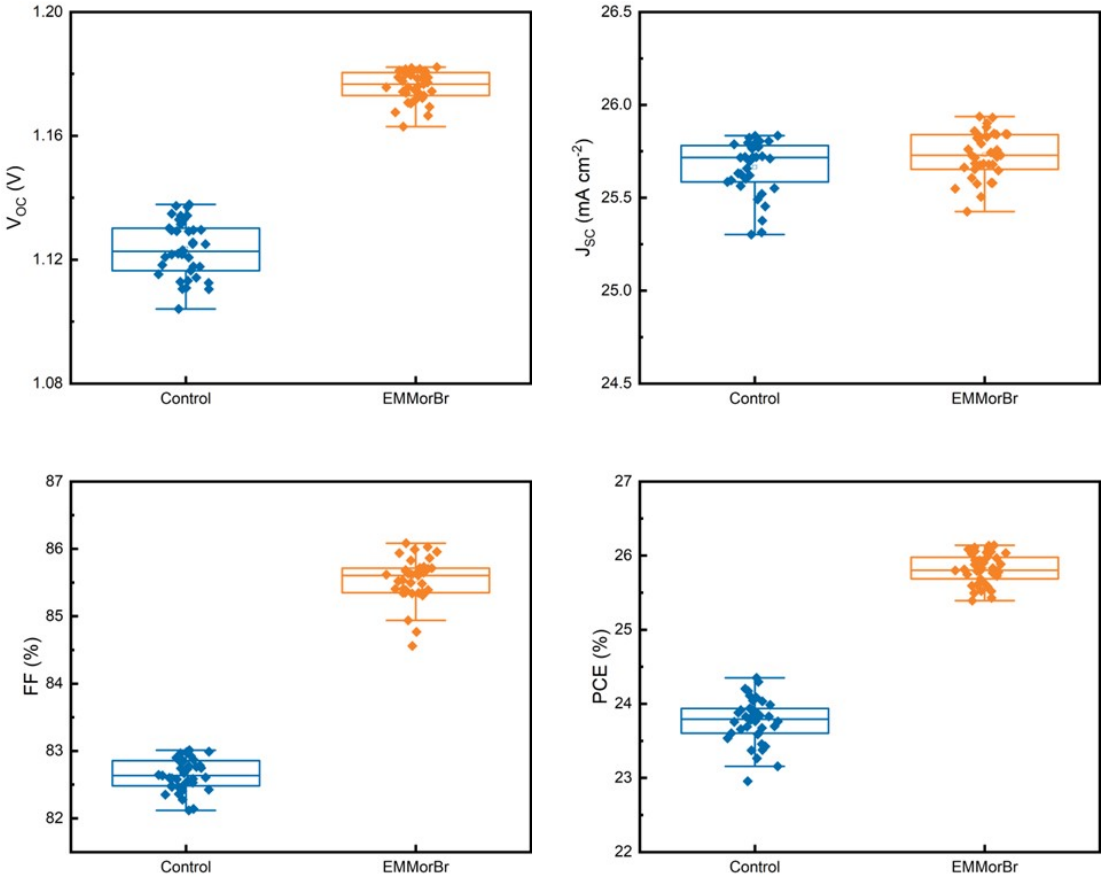

Fig S14. Statistics of V_{OC}, J_{SC}, FF and PCE of the PSCs modulated by different concentrations of EMMorBr. The statistic data were obtained from individual 38 devices for each kind of PSCs.

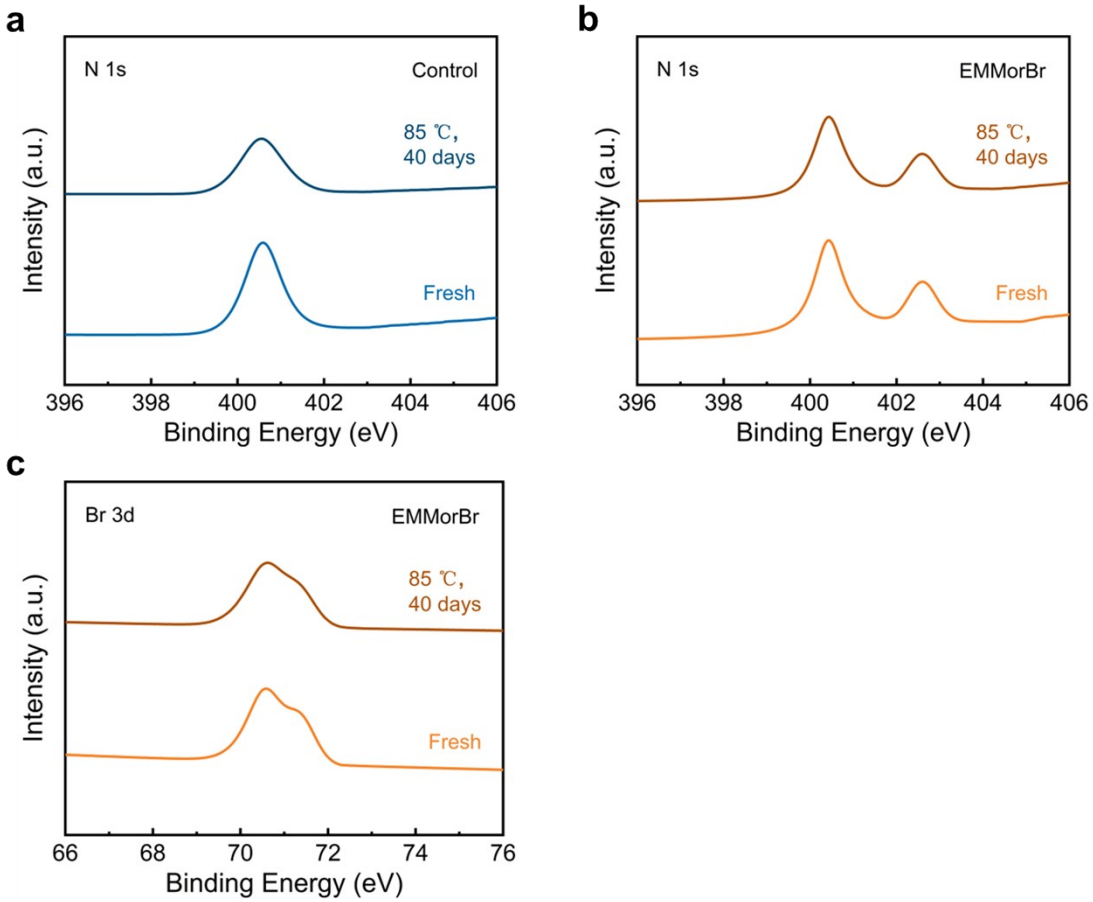

Fig S15. Comparisons of XPS N1s signals between fresh and aged (at 85 °C for 40 days) perovskite thin films without (a) and with (b) EMMorBr passivation. (c) Br 3d signals between fresh and aged EMMorBr-modified films.

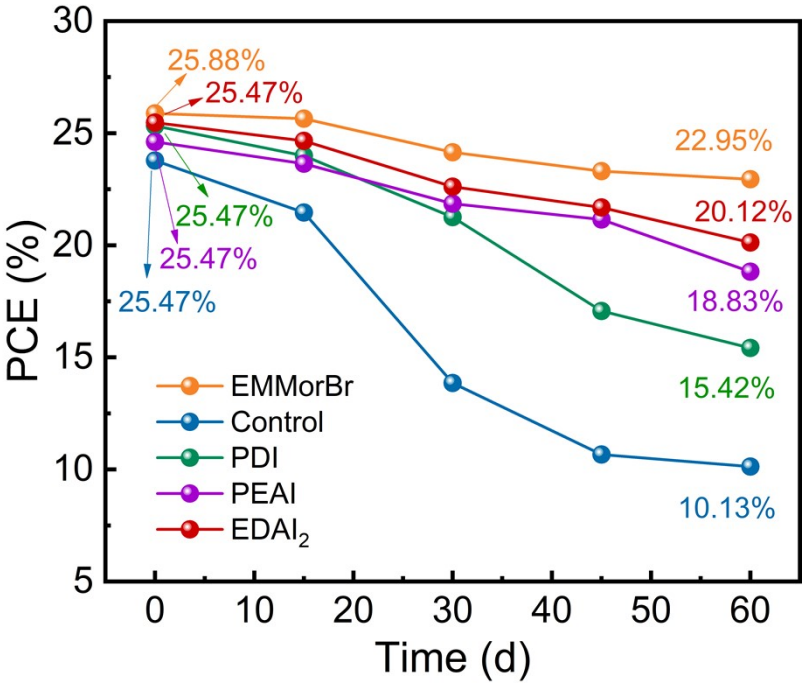

Fig S16. Comparison of efficiency and stability between EMMorBr and common passivators, average PCE based on 12 devices.

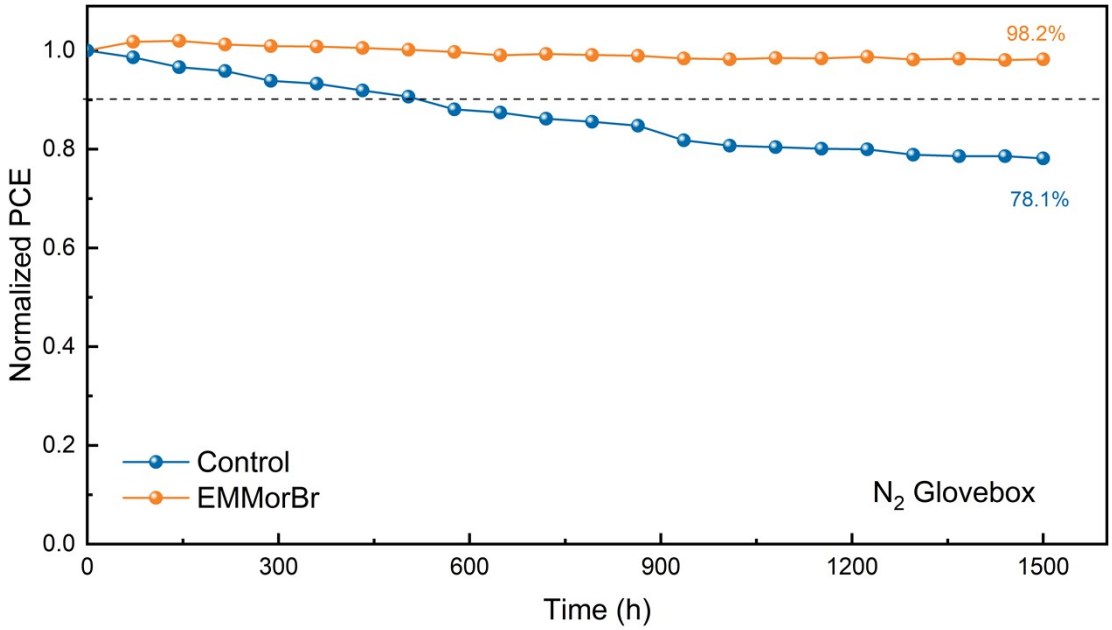

Fig S17. Evolution of PCE measured from the unencapsulated PSCs for 1500 h under N_2 atmosphere.

Table S1. Fitting data of TRPL curves in **Fig. 3f** based on double exponential function

Samples	τ_1 (μs)	A_1 (%)	τ_2 (μs)	A_2 (%)	τ_{avg} (μs)
Control	0.20	3.59	1.96	96.41	1.96
EMMorBr	0.29	1.56	2.18	98.44	2.18

Table S2. Photovoltaic parameters of the PSCs based on the control and EMMorBr-treated 1.55 eV PSCs.

Samples	V_{OC} (V)	J_{SC} (mA cm^{-2})	FF (%)	PCE (%)	HI (%)
Control-FS	1.124	25.75	79.70	23.07	5.26
Control-RS	1.137	25.80	82.99	24.35	
EMMorBr-FS	1.179	25.76	85.23	25.87	1.03
EMMorBr-RS	1.181	25.84	85.67	26.14	

Table S3. EIS fitting parameters of PSCs with and without EMMorBr treatment.

Samples	R_S (Ω)	R_{rec} (Ω)	C_{rec} (F)
Control	20.13	1832.06	1.95×10^{-8}
EMMorBr	13.29	2833.17	1.74×10^{-8}